A Parameterization for the Absorption of Solar Radiation by Water Vapor in the Earth's Atmosphere

WEI-CHYUNG WANG

Goddard Institute for Space Studies, NASA, New York, N. Y. 10025

(Manuscript received 11 November 1974, in revised form 23 September 1975)

ABSTRACT

A parameterization for the absorption of solar radiation as a function of the amount of water vapor in the earth's atmosphere is obtained. Absorption computations are based on the Goody band model and the near-infrared absorption band data of Ludwig *et al.* A two-parameter Curtis-Godson approximation is used to treat the inhomogeneous atmosphere. Heating rates based on a frequently used one-parameter pressure-scaling approximation are also discussed and compared with the present parameterization.

1. Introduction

A simple but reliable treatment for the absorption of solar radiation in the earth's atmosphere has essential application in numerical circulation models and in other atmospheric studies. Such application generally requires a parameterized form for the absorption rates based on more detailed and more time-consuming calculations.

The principal gaseous absorbers in the earth's atmosphere are water vapor in the troposphere and ozone in the stratosphere. Sasamori *et al.* (1972) give a simple parameterization for absorption by carbon dioxide and oxygen, which are minor contributors to the total atmospheric absorption. The stratospheric heating due to ozone can be accurately parameterized because ozone absorption can be treated as exponential attenuation at each wavelength with negligible temperature and pressure dependence (Lacis and Hansen, 1974). However, absorption by water vapor is more difficult to parameterize because the absorption spectrum is complicated and depends strongly on temperature and pressure.

Formulations for water vapor absorption in recent use (Korb *et al.*, 1956; McDonald, 1960; Yamamoto, 1962; Sasamori *et al.*, 1972) are based on the near-infrared total band measurements of Howard *et al.* (1956), including the measurements by Fowle (1915) for the weak absorption bands near 0.7 and 0.8 μm which were not measured by Howard *et al.* These parameterizations employ a one-parameter pressure-scaling (PS) approximation to account for the atmospheric inhomogeneity. This may be adequate over a limited region of the atmosphere as demonstrated by aircraft measurements of the net solar flux in the lower atmosphere made by Paltridge (1973). However, as noted by Goody (1964a), the one-parameter approximation is not sufficient to give accurate results over the whole atmosphere. Better results can be obtained with a two-parameter approximation (cf. Goody, 1964a). Kaplan (1959), Walshaw and Rogers (1963) and Goody (1964b) have studied the Curtis-Godson (CG) approximation and concluded that this method is accurate for water vapor over a wide range of conditions.

In the present study, we use the measurements compiled by Ludwig *et al.* (1973) and the CG approximation in conjunction with narrow-band model analysis to obtain a reliable parameterization for water vapor absorption in the earth's atmosphere.

2. Analysis

a. Spectral data

Ferriso *et al.* (1966) and Ludwig (1971) measured the curve-of-growth of water vapor in the 1–10 μm region. They obtained the mean absorption coefficient S_E and mean line spacing d averaged over 25 cm^{-1} intervals by fitting the measurements with the Goody narrow-band model and a collision-broadened half-width b. The line half-width b used by Ferriso *et al.* (1966) is

$$b=(0.09P_{H_2O}+0.09P_{N_2}+0.04P_{O_2})\left(\frac{273}{T}\right)^{\frac{1}{2}}+0.44P_{H_2O}\left(\frac{273}{T}\right), \quad (1)$$

where P_{H_2O}, P_{N_2} and P_{O_2} are the partial pressures (atm) of water vapor, nitrogen and oxygen. The self-broadening effect of water vapor is included in the first term to account for non-resonant collisions; the second term accounts for resonant collisions which have a different temperature dependence.

TABLE 1. Band model parameters S_E (cm-atm)$^{-1}_{STP}$ and B_E computed by averaging McClatchey *et al.* (1973) line data over 25 cm^{-1}.*

ν(cm^{-1})	S_E(200 K)	S_E(250 K)	S_E(296 K)	B_E(200 K)	B_E(250 K)	B_E(296 K)
8300	1.07E-04	9.86E-05	9.26E-05	.055	.055	.055
8325	6.11E-05	5.62E-05	5.39E-05	.056	.055	.056
8350	9.77E-05	8.26E-05	7.42E-05	.061	.063	.067
8375	6.95E-05	6.11E-05	5.68E-05	.057	.061	.055
8400	6.55E-05	6.03E-05	5.80E-05	.066	.070	.073
8425	1.39E-04	1.16E-04	1.04E-04	.058	.062	.065
8450	2.15E-04	1.89E-04	1.77E-04	.075	.077	.078
8475	7.83E-05	7.63E-05	7.62E-05	.047	.052	.056
8500	8.35E-05	9.13E-05	1.01E-04	.051	.058	.065
8525	7.47E-05	9.20E-05	1.14E-04	.079	.088	.092
8550	5.24E-05	7.82E-05	1.17E-04	.092	.095	.090
8575	4.42E-05	1.00E-04	1.89E-04	.110	.100	.090
8600	6.43E-05	1.68E-04	3.13E-04	.081	.067	.061
8625	2.70E-04	5.62E-04	8.84E-04	.069	.061	.057
8650	5.91E-04	1.10E-03	1.46E-03	.063	.062	.062
8675	1.22E-03	1.84E-03	2.22E-03	.055	.051	.049
8700	1.72E-03	1.99E-03	2.14E-03	.056	.054	.052
8725	4.39E-03	4.36E-03	4.26E-03	.045	.043	.042
8750	3.69E-03	3.19E-03	2.87E-03	.038	.038	.040
8775	3.08E-03	2.42E-03	2.06E-03	.026	.028	.030
8800	5.43E-03	5.87E-03	5.57E-03	.060	.065	.069
8825	4.99E-03	5.13E-03	5.48E-03	.078	.078	.076
8850	5.49E-03	4.20E-03	3.52E-03	.036	.039	.042
8875	8.90E-03	7.40E-03	6.55E-03	.052	.051	.051
8900	6.39E-03	6.27E-03	6.08E-03	.060	.059	.058
8925	4.35E-03	5.30E-03	5.91E-03	.076	.070	.067
8950	1.47E-03	2.07E-03	2.58E-03	.069	.060	.055
8975	5.70E-04	9.51E-04	1.37E-03	.084	.073	.064
9000	1.40E-04	3.35E-04	5.95E-04	.077	.061	.055
9025	2.47E-04	2.49E-04	3.02E-04	.071	.085	.084
9050	2.54E-04	2.48E-04	2.71E-04	.086	.097	.103
9075	2.14E-04	2.20E-04	2.26E-04	.083	.082	.082
9100	1.94E-04	1.96E-04	2.03E-04	.087	.090	.089
9125	8.53E-05	8.99E-05	9.64E-05	.054	.061	.063
9150	3.69E-05	8.64E-05	8.86E-05	.031	.036	.038
9175	5.84E-05	6.24E-05	6.54E-05	.043	.044	.045
9200	5.53E-05	6.20E-05	6.58E-05	.023	.023	.023
9225	2.65E-05	3.27E-05	3.74E-05	.026	.027	.027
9250	2.33E-05	3.35E-05	4.18E-05	.035	.032	.031
9275	1.09E-05	1.31E-05	2.49E-05	.037	.034	.032
9300	4.74E-06	1.00E-05	1.57E-05	.027	.025	.024
9325	3.94E-06	6.83E-06	1.02E-05	.031	.030	.023
9350	1.33E-06	3.33E-06	6.19E-06	.036	.031	.027
9375	7.17E-07	1.39E-06	2.35E-06	.029	.027	.024
9400	4.10E-07	8.16E-07	1.26E-06	.010	.010	.010
9425	2.46E-07	4.33E-07	6.24E-07	.015	.013	.011
9450	5.93E-07	1.99E-06	3.82E-06	.013	.010	.009
9475	1.07E-07	1.71E-07	2.32E-07	.016	.016	.015
9500	5.98E-08	1.24E-07	1.97E-07	.006	.005	.004
9525	2.15E-09	4.45E-09	6.84E-09	.003	.002	.002
9550	2.79E-08	5.53E-08	8.59E-08	.019	.017	.015
9575	1.20E-08	1.81E-08	2.33E-08	.006	.005	.005
9600	2.29E-08	4.47E-08	6.85E-08	.014	.011	.010
9625	5.40E-09	7.98E-09	9.93E-09	.004	.004	.004
9650	2.45E-08	5.69E-08	9.76E-08	.007	.005	.004
9675	8.40E-08	1.71E-07	2.60E-07	.009	.008	.007
9700	3.01E-07	4.95E-07	6.68E-07	.014	.012	.011
9725	1.72E-06	2.17E-06	2.48E-06	.024	.023	.022
9750	1.02E-06	1.10E-06	1.13E-06	.025	.023	.022
9775	5.66E-06	5.30E-06	5.04E-06	.035	.032	.030
9800	3.90E-06	3.31E-06	2.96E-06	.026	.024	.023
9825	1.35E-06	1.32E-06	1.31E-06	.022	.021	.020
9850	3.06E-06	2.41E-06	2.08E-06	.019	.019	.018
9875	3.80E-06	3.03E-06	2.62E-06	.019	.019	.019
9900	9.52E-06	7.87E-06	6.86E-06	.041	.038	.035
9925	4.04E-06	3.60E-06	3.32E-06	.022	.022	.022
9950	4.95E-06	5.00E-06	4.99E-06	.025	.025	.025
9975	4.79E-06	5.29E-06	5.64E-06	.053	.051	.049
10000	1.51E-06	1.54E-06	1.61E-06	.015	.016	.016
10025	1.61E-06	1.90E-06	2.11E-06	.020	.020	.020
10050	5.12E-07	8.10E-07	1.25E-06	.026	.026	.024
10075	1.35E-06	2.20E-06	3.54E-06	.040	.042	.040
10100	1.66E-06	3.38E-06	5.86E-06	.056	.050	.043
10125	2.07E-06	5.63E-06	1.07E-05	.051	.042	.037
10150	7.24E-06	1.52E-05	2.41E-05	.050	.043	.040
10175	3.60E-05	5.61E-05	7.40E-05	.048	.047	.046
10200	4.53E-05	6.27E-05	7.62E-05	.047	.045	.044
10225	7.18E-05	8.58E-05	9.54E-05	.054	.052	.051
10250	2.35E-04	2.26E-04	2.20E-04	.047	.049	.053
10275	1.16E-04	1.09E-04	1.08E-04	.052	.057	.062
10300	1.34E-04	1.11E-04	1.06E-04	.029	.035	.041
10325	9.50E-05	8.17E-05	8.28E-05	.040	.054	.062
10350	2.78E-04	2.65E-04	2.77E-04	.081	.089	.092
10375	3.45E-04	3.48E-04	3.86E-04	.077	.090	.092
10400	4.52E-04	4.87E-04	5.55E-04	.074	.078	.076
10425	3.86E-04	5.17E-04	6.46E-04	.109	.102	.094
10450	4.30E-04	6.08E-04	7.52E-04	.082	.073	.066
10475	6.82E-04	9.01E-04	1.06E-03	.076	.070	.067

* Tabular entries for S_E include exponent of 10 factor, i.e., 1.07E–04 = 1.07×10^{-4}.

TABLE 1 (*continued*)

ν(cm^{-1})	S_E(200 K)	S_E(250 K)	S_E(296 K)	B_E(200 K)	B_E(250 K)	B_E(296 K)
10500	1.04E-03	1.19E-03	1.27E-03	.070	.067	.066
10525	1.65E-03	1.63E-03	1.61E-03	.051	.055	.058
10550	1.33E-03	1.29E-03	1.31E-03	.057	.063	.067
10575	1.62E-03	1.65E-03	1.70E-03	.060	.058	.055
10600	3.82E-03	3.36E-03	3.06E-03	.052	.050	.048
10625	9.52E-04	7.51E-04	6.42E-04	.049	.051	.052
10650	2.32E-03	1.76E-03	1.45E-03	.037	.039	.040
10675	4.07E-03	3.48E-03	3.10E-03	.068	.067	.067
10700	3.45E-03	3.58E-03	3.61E-03	.067	.067	.067
10725	1.21E-03	1.62E-03	1.94E-03	.081	.076	.073
10750	4.05E-04	7.01E-04	1.01E-03	.088	.084	.080
10775	1.02E-04	1.40E-04	2.02E-04	.125	.135	.130
10800	7.01E-05	7.11E-05	7.88E-05	.083	.094	.097
10825	6.42E-05	7.35E-05	8.42E-05	.094	.093	.089
10850	5.92E-05	6.87E-05	7.98E-05	.079	.079	.074
10875	7.64E-05	9.50E-05	1.12E-04	.065	.064	.062
10900	1.40E-04	1.57E-04	1.70E-04	.114	.108	.102
10925	2.01E-04	2.05E-04	2.09E-04	.115	.113	.110
10950	2.60E-04	2.60E-04	2.58E-04	.077	.080	.081
10975	3.07E-04	2.92E-04	2.87E-04	.076	.077	.076
11000	2.93E-04	2.87E-04	2.85E-04	.078	.077	.075
11025	2.97E-04	2.53E-04	2.27E-04	.045	.045	.045
11050	8.75E-05	7.64E-05	7.08E-05	.043	.044	.044
11075	3.89E-04	3.04E-04	2.58E-04	.038	.039	.039
11100	3.55E-04	3.18E-04	2.94E-04	.062	.063	.063
11125	3.67E-04	3.78E-04	3.81E-04	.050	.049	.048
11150	1.32E-04	1.79E-04	2.15E-04	.058	.054	.051
11175	3.59E-05	6.39E-05	9.32E-05	.045	.045	.044
11200	1.00E-05	1.55E-05	2.35E-05	.042	.044	.042
11225	1.31E-06	2.04E-06	3.29E-06	.022	.025	.023
11250	1.59E-06	1.80E-06	1.92E-06	.019	.017	.015
11275	1.82E-06	2.02E-06	2.12E-06	.020	.018	.016
11300	2.95E-07	4.32E-07	5.39E-07	.020	.018	.017
11325	5.01E-07	7.75E-07	1.02E-06	.028	.024	.021
11350	3.39E-07	5.48E-07	7.34E-07	.021	.020	.019
11375	1.14E-07	2.33E-07	3.73E-07	.031	.030	.029
11400	4.14E-08	7.30E-08	1.09E-07	.013	.012	.011
11425	2.05E-08	5.30E-08	9.46E-08	.008	.008	.007
11450	1.73E-08	3.24E-08	4.76E-08	.008	.006	.005
11475	4.30E-09	1.27E-08	2.49E-08	.004	.004	.004
11500	3.81E-09	8.49E-09	1.38E-08	.006	.005	.005
11525	4.90E-09	1.06E-08	1.75E-08	.009	.008	.007
11550	0.0	0.0	0.0	.0	.0	.0
11575	1.58E-08	3.37E-08	5.91E-08	.010	.007	.005
11600	3.69E-08	8.75E-08	1.50E-07	.010	.008	.006
11625	1.48E-08	2.38E-08	3.78E-08	.012	.011	.009
11650	3.94E-07	7.42E-07	1.08E-06	.018	.017	.016
11675	4.09E-07	6.44E-07	8.61E-07	.030	.028	.026
11700	2.24E-06	2.81E-06	3.20E-06	.026	.024	.023
11725	2.74E-06	2.94E-06	3.03E-06	.032	.031	.031
11750	5.11E-06	4.89E-06	4.73E-06	.033	.033	.032
11775	3.12E-06	2.58E-06	2.28E-06	.022	.022	.022
11800	2.16E-06	1.87E-06	1.79E-06	.022	.026	.028
11825	3.64E-06	2.93E-06	2.64E-06	.028	.031	.033
11850	6.32E-06	5.26E-06	4.81E-06	.034	.037	.039
11875	7.44E-06	6.50E-06	6.33E-06	.038	.041	.043
11900	9.43E-06	1.02E-05	1.17E-05	.057	.063	.065

Ferriso *et al.* (1966) give an empirical relation for the temperature dependence of the band-averaged line spacing for the vibrational-rotational bands:

$$\bar{d}(T)=\exp(1.21-0.00106T). \qquad (2)$$

Ludwig and Ferriso (1967) compared the total band emissivities based on these narrow band parameters with available experimental data and found satisfactory agreement.

Because the Ludwig *et al.* data extend only to 9300 cm^{-1}, additional data are needed for the 0.7, 0.8, 0.9 and 1.1 μm bands. We use the water vapor line parameters compiled by McClatchey *et al.* (1973) for the 0.9 and 1.1 μm bands and transmission measurements by Fowle (1915) for the 0.7 and 0.8 μm bands.

Band model parameters can be obtained directly from line data by appropriately averaging the line strengths and line widths (cf. Goody, 1964a; Goldman and Kyle, 1968):

$$s=\sum_i s_i, \qquad (3)$$

$$b=\frac{1}{s}\Big[\sum_i (b_i s_i)^{\frac{1}{2}}\Big]^2, \qquad (4)$$

where the s_i and b_i are individual line intensities and line widths, respectively. The temperature dependence of the line intensities is included through the Boltzmann factor and the vibrational-rotational partition function. The band model parameters $S_E=s/d$ and $B_E=b/d$ averaged over 25 cm^{-1} intervals are computed for 200, 250 and 296 K and are shown in Table 1.

For the 0.7 and 0.8 μm bands, the mean absorption coefficients are derived by fitting the measured transmission with the Goody band model using the mean line half-width and the band-averaged line spacing

TABLE 2. Values of S_E (cm-atm)$^{-1}_{STP}$ of the 0.7 and 0.8 μm bands.

Band fraction	Band 0.7 μm (13 500–14 300 cm^{-1})	0.8 μm (11 900–12 650 cm^{-1})
0.2	3.13E–05	3.60E–05
0.8	3.88E–05	3.78E–05

relations given in (1) and (2) for a standard pressure (1013 mb) and temperature (273 K). Two values of S_E are used to fit the measured transmission for each band. The mean absorption coefficients S_E thus obtained for the 0.7 and 0.8 μm bands are listed in Table 2. The accuracy of the fit is within $\sim 2\%$ of Fowle's transmission measurements for the interval $0.2 \leqslant u \leqslant 8.0$ cm, where u is the precipitable water vapor amount.

The band model parameters derived from fitting the curve-of-growth (Ludwig *et al.* data) should give an accurate representation for the absorption by water vapor including also the contribution by water vapor continuum. However, it should be cautioned that band model parameters derived directly from line data by relations (3) and (4) may require further comparison with measurements (cf. Goldman and Kyle, 1968).

b. Inhomogeneous atmosphere

For a clear sky, the directly transmitted solar flux at a height z for a solar zenith angle $\theta_0 = \cos^{-1}\mu_0$ is

$$F^t_{\Delta\nu} = \mu_0 F^0_{\Delta\nu} T_{\Delta\nu}(x), \tag{5}$$

where $F^0_{\Delta\nu}$ is the incident solar flux in the frequency interval $\Delta\nu$ at the top of the atmosphere ($z = z_\infty$), and $T_{\Delta\nu}$ the transmission function defined by

$$T_{\Delta\nu}(x) = \frac{1}{\Delta\nu}\int_{\Delta\nu} \exp\left(-\int_0^x k_\nu du\right) d\nu. \tag{6}$$

Here $x = u/\mu_0$, where u is the water vapor amount in a vertical column between z and z_∞, and k_ν the spectral absorption coefficient.

Similarly, at the height z, the solar flux reflected by the ground is given by

$$F^r_{\Delta\nu} = R_s \mu_0 F^0_{\Delta\nu} T_{\Delta\nu}(x^*), \tag{7}$$

where R_s is the surface albedo,

$$x^* = u^0/\mu_0 + (u^0 - u)/\bar{\mu} \tag{8}$$

is the total absorber amount traversed by the diffuse reflected radiation, u^0 is the total absorber amount in a vertical column of the earth's atmosphere, and $\bar{\mu} = \frac{3}{5}$ is the diffusivity factor for the reflected radiation.

In the CG approximation, the inhomogeneous path through the atmosphere is replaced by an equivalent homogeneous path that has the same transmission (cf. Goody, 1964a; Tien, 1968). The approximation is exact in the strong and weak line limits. For the Goody band model, the transmission function is

$$T_{\Delta\nu}(x) = \exp\left[\frac{-\langle S_E\rangle x}{\left(1 + \dfrac{\langle S_E\rangle x}{4\langle B_E\rangle}\right)^{\frac{1}{2}}}\right], \tag{9}$$

where $\langle S_E\rangle$ is the effective mean absorption coefficient

$$\langle S_E\rangle = \frac{1}{u}\int_0^u S_E du, \tag{10}$$

and $\langle B_E\rangle$ the effective mean line half-width-to-line-spacing ratio

$$\langle B_E\rangle = \frac{1}{\langle S_E\rangle u}\int_0^u S_E B_E du. \tag{11}$$

The terms inside the integrals are evaluated for locally homogeneous conditions corresponding to the local temperature and pressure. The CG approximation has been studied by Kaplan (1959), Walshaw and Rogers (1963) and Goody (1964a), and found to be accurate for water vapor. Krakow *et al.* (1966) have also examined the CG approximation and found excellent agreement with the measured transmittance.

In the PS approximation, the inhomogeneous path is accounted for by scaling the water vapor amount according to

$$\langle u\rangle = u\left(\frac{P}{P_0}\right)^n \left(\frac{T_0}{T}\right)^{\frac{1}{2}}, \tag{12}$$

where P_0 and T_0 are the standard pressure and temperature, and the value of n is between 0 and 1.0. The square-root temperature scaling is included, but the effect is small. The resulting transmission function for the PS approximation is

$$T_{\Delta\nu}(x) = \exp\left[\frac{-S_E\langle x\rangle}{\left(1 + \dfrac{S_E\langle x\rangle}{4B_E}\right)^{\frac{1}{2}}}\right]. \tag{13}$$

As indicated in Goody (1964a), this one-parameter method is practically equivalent to assuming no temperature variation of absorption at all. Furthermore the scaling parameter n actually depends on the product of $S_E u$; thus a fixed value of n used to scale the water vapor amount can be expected to yield large errors when applied over broad spectral regions.

The net solar flux at the height z is given by

$$F = \sum_i \mu_0 F^0_{\Delta\nu_i} [T_{\Delta\nu_i}(x) - R_s T_{\Delta\nu_i}(x^*)], \tag{14}$$

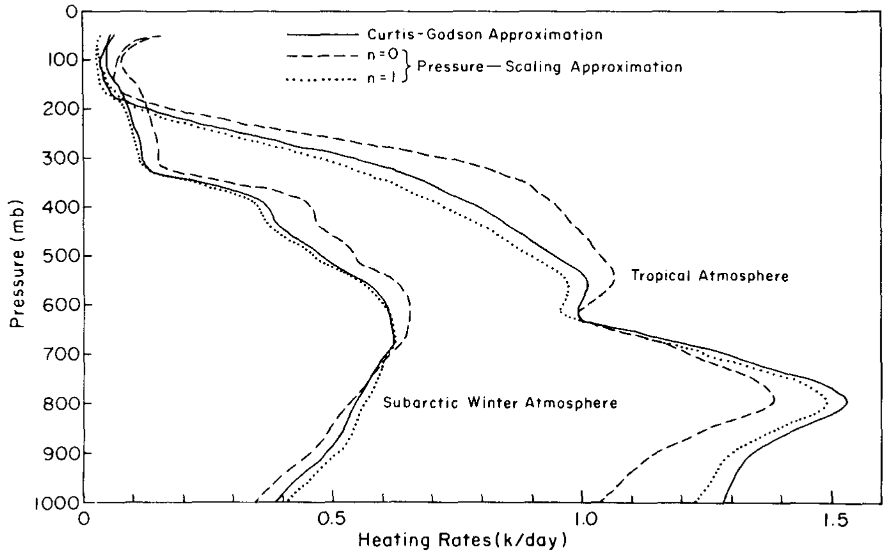

FIG. 1. Heating rates due to water vapor absorption for tropical and subarctic winter atmospheres of McClatchey *et al.*, (1972) with solar zenith angle $\theta_0=60°$ and ground albedo $R_s=0.07$. The solid line shows heating rates computed with the Curtis-Godson approximation [Eqs. (9), (10), (11), (15)]. The dashed and dotted lines depict the pressure-scaling approximation with $n=0$ and $n=1$, respectively [Eqs. (12), (13), (15)].

and the corresponding atmospheric heating rate is

$$\frac{\Delta T}{\Delta t}=\frac{g\Delta F}{c_p\Delta P\Delta t}, \tag{15}$$

where c_p is the specific heat at constant pressure, g the gravitational acceleration, and ΔF the difference of net solar flux at the top and bottom of a layer with pressure difference ΔP.

We define the atmospheric absorptivity for water vapor for the case of normal incidence ($\mu_0=1$):

$$A(u)=1-\sum_i T_{\Delta\nu_i}(u)F^0_{\Delta\nu_i}/\sum_i F^0_{\Delta\nu_i}, \tag{16}$$

where the spectral dependence of the solar flux is taken from Labs and Neckel (1968).

3. Results

Fig. 1 shows the clear sky heating rates based on the CG approximation. Also included for comparison is the narrow-band PS approximation with $n=0$ and 1.0. The illustrations are for tropical and subarctic winter models (McClatchey *et al.*, 1972) for a solar zenith angle $\theta_0=60°$ and surface albedo $R_s=0.07$, which is representative of the mean ocean albedo. The amount of precipitable water vapor in the atmosphere is 4.15 and 0.42 cm for the tropical and subarctic winter cases; the scaled water vapor amounts are 4.03 (3.30) cm and 0.44 (0.33) cm for $n=1$ ($n=0$). The results show that the main effect of pressure scaling is to reduce the heating rates at high altitudes and to increase the heating rates at low altitudes. It is also interesting to note that the difference between no scaling and linear scaling is not necessarily a measure of the uncertainty due to the PS approximation. For example, the PS approximation for both $n=0$ and $n=1$ yields less heating than the CG approximation at low altitudes of the tropical model because of the reduced effective water vapor amount in the lower atmosphere. However, if applied to narrow-band intervals, the PS approximation with $n=0.9$ can yield results of comparable accuracy to the CG approximation over much of the atmosphere.

It is possible to obtain a reliable atmospheric absorptivity based on computations for a mean water vapor profile if the *relative* vertical distribution of water vapor in the atmosphere does not differ greatly from day to day. For this purpose we use the tropical model of McClatchey *et al.* (1972) both for the water vapor profile and for the pressure and temperature distributions. The analytic expression

$$\log_{10}A(u)=-1.1950+0.4459\log_{10}u-0.0345(\log_{10}u)^2 \tag{17}$$

fits the computed results from (9)–(11) and (16) within 0.3% over the absorber interval $0.008\leqslant u\leqslant 4.15$ cm. Since the pressure and temperature effects on absorption have been incorporated in the CG approximation, u in (17) refers to standard pressure and temperature (i.e., u is the actual water vapor content of the atmosphere in precipitable centimeters). Note that the parameterization in (17) includes the effect of atmospheric inhomogeneity and is appropriate for computing atmospheric heating rates rather than absorption along horizontal (homogeneous) paths.

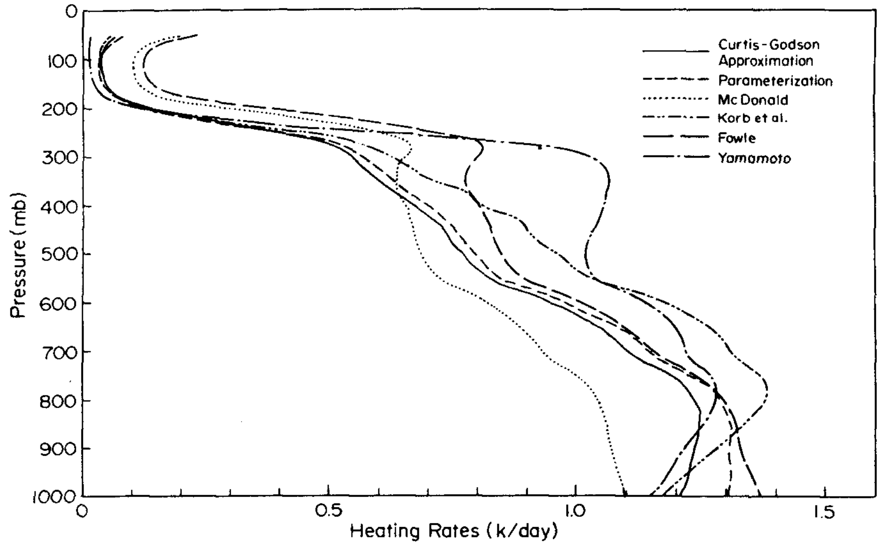

FIG. 2. Heating rates due to water vapor absorption from the mid-latitude summer atmosphere of McClatchey *et al.* (1972) with solar zenith angle $\theta_0=60°$ and ground albedo $R_s=0.07$. The Curtis-Godson computations are shown by the solid line. The parameterized heating rates (dashed line) are computed from (18). Heating rates based on absorptivities due to Fowle (1915), Korb *et al.* (1952), McDonald (1960) and Yamamoto (1962) are computed with the pressure-scaling approximation with $n=1$.

Atmospheric heating rates for the parameterized absorptivity (17) are computed by

$$\frac{\Delta T}{\Delta t}=\frac{g\mu_0F^0}{c_p\Delta P\Delta t}\{A(x+\Delta x)-A(x)+R_s[A(x^*)-A(x^*+\Delta x^*)]\},\qquad(18)$$

where F^0 ($=1365$ W m^{-2}) is the solar constant and Δu ($=\mu_0\Delta x$) is the absorber amount in the pressure interval ΔP. The accuracy of the heating rates obtained with (18) is within $\sim$1.8% of the narrow-band CG calculations over the same fitting interval.

Next we examine the accuracy of (18) for atmospheric conditions that are different from those used in the derivation of (17). Fig. 2 illustrates the heating rates for the mid-latitude summer model of McClatchey *et al.* (1972) with solar zenith angle 60° and ground albedo 0.07; the water vapor content is 2.95 cm. Because of the slant path, the effective water vapor amount is outside the fitting interval for this case. However, the agreement with the CG approximation is still satisfactory.

Also illustrated in Fig. 2 are heating rates based on the PS approximation with $n=1.0$ for the water

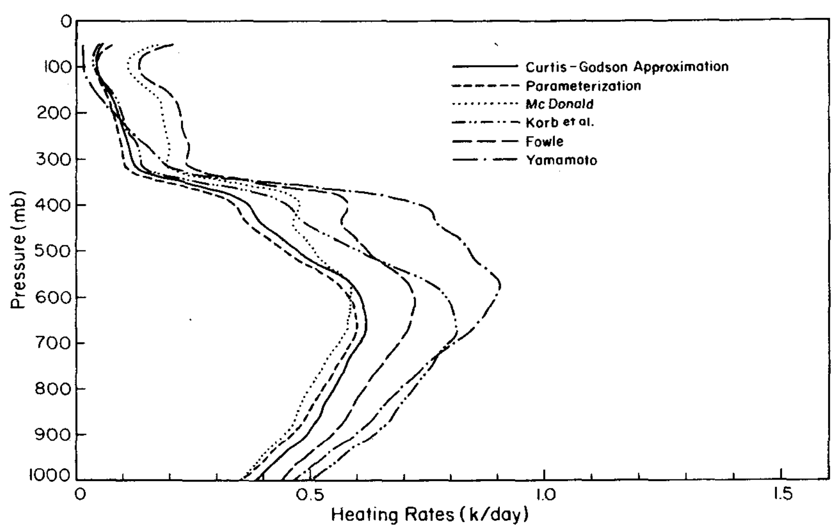

FIG. 3. As in Fig. 2 except for the subarctic winter atmosphere.

vapor absorptivities of Fowle (1915), Korb *et al.* (1956), McDonald (1960) and Yamamoto (1962). Part of the discrepancy between the different heating rates is due to the absorption data used. For example, Fowle's and McDonald's absorptivities differ from each other by 20–30% because two different sets of Smithsonian solar absorption data were used. The heating rates of Korb *et al.* and Yamamoto are less consistent in middle and high altitudes even though both used the Howard *et al.* data. The interesting feature is the bulge in Yamamoto's curve near ~400 mb while the curve for Korb *et al.* is closer to the CG approximation. This may be attributed to the interpolation scheme used by Korb *et al.* to account for the inhomogeneous atmosphere. Below ~400 mb, the present parameterization gives heating rates that lie between Fowle's and McDonald's curves; at high altitudes, the present parameterization is in better agreement with the Korb *et al.* and Yamamoto formulations. However, considering the whole atmosphere, all of these previous absorptivities show large departures from the CG results.

Fig. 3 repeats the calculations for the subarctic winter atmosphere of McClatchey *et al.* (1972), and compares the accuracy of the different absorption formulas for the case of a small amount of atmospheric water vapor. The overall agreement between the present parameterization and the CG approximation is again very good. The relative differences among the heating rates for the other absorptivities are similar to the mid-latitude summer case. The present results agree well with McDonald's heating rates, but are substantially smaller than Yamamoto's and Korb *et al.*'s heating rates in the lower atmosphere. This may be due to Yamamoto's extrapolation of the absorptivity for small values of water vapor amount (cf. Yamamoto, 1962).

Finally, we check the accuracy of the present parameterization for the case of high surface albedo. Instead of $R_s=0.07$ adopted for the two examples shown, we use $R_s=0.25$ (representative value of the albedo of land) for the mid-latitude summer atmosphere and $R_s=0.80$ (value of the albedo of snow-covered ground) for the subarctic winter atmosphere. The overall agreement with the CG approximation is similar to the illustrated low-albedo cases.

In summary, the present parameterization for the absorption by water vapor gives satisfactory heating rates over the whole atmosphere compared to the detailed narrow-band calculations. The pressure and temperature dependence of the water vapor absorption is incorporated through the CG approximation so that pressure scaling of the water vapor amount is no longer required.

Acknowledgments. I am indebted to Dr. A. A. Lacis for his helpful comments and careful reading of the manuscript. The work was done while the author held a NAS-NRC resident research associateship at the Goddard Institute for Space Studies.

REFERENCES

Ferriso, C. C., C. B. Ludwig and A. L. Thomson, 1966: Empirically determined infrared absorption coefficients of H_2O from 300 to 3000°K. *J. Quant. Spectros. Radiat. Transfer*, **6**, 241–275.

Fowle, F. E., 1915: The transparency of aqueous vapor. *Astrophys. J.*, **42**, 394–411.

Goldman, A., and T. G. Kyle, 1968: A comparison between statistical model and line by line calculation with application to the 9.6-μ ozone and the 2.7-μ water vapor bands. *Appl. Opt.*, **7**, 1167–1177.

Goody, R. M., 1964a: *Atmospheric Radiation.* Oxford University Press, 436 pp.

——, 1964b: The transmission of radiation through an inhomogeneous atmosphere. *J. Atmos. Sci.*, **21**, 575–581.

Howard, J. N., D. E. Burch and D. Williams, 1956: Infrared transmission of synthetic atmospheres, Parts I–V. *J. Opt. Soc. Amer.*, **46**, 186–190, 237–241, 242–245, 334–338, 452–455.

Kaplan, L. D., 1959: A method for calculation of infrared flux for use in numerical models of atmospheric motion. *The Atmosphere and the Sea in Motion*, Rockefeller Institute Press and Oxford University Press, 170–177.

Korb, G., J. Michalowsky and F. Möller, 1956: Investigations on the heat balance of the troposphere. AFCRL Tech. Note TN-56-881, 94 pp.

Krakow, B., H. J. Babrov, G. J. Maclay and A. L. Shabott, 1966: Use of Curtis-Godson approximation in calculation of radiant heating by inhomogeneous hot gases. *Appl. Opt.*, **5**, 1791–1800.

Labs, D., and H. Neckel, 1968: The radiation of the solar photosphere from 2000 Å to 100 μ. *Z. Astrophys.*, **69**, 1–73.

Lacis, A. A., and J. E. Hansen, 1974: A parameterization for the absorption of solar radiation in the earth's atmosphere. *J. Atmos. Sci.*, **31**, 118–133.

Ludwig, C. B., 1971: Measurements of the curves-of-growth of hot water vapor. *Appl. Opt.*, **10**, 1057–1073.

——, and C. C. Ferriso, 1967: Prediction of total emissivity of nitrogen-broadened and self-broadened hot water vapor. *J. Quant. Spectros. Radiat. Transfer*, **7**, 7–26.

——, W. Malkmus, J. E. Reardon and J. A. L. Thomson, 1973: *Handbook of Infrared Radiation from Combustion Gases.* NASA SP-3080, 486 pp.

McClatchey, R. A., R. W. Fenn, J. E. Selby, F. E. Volz and J. S. Garing, 1972: Optical properties of the atmosphere, 3rd ed. AFCRL Environ. Res. Papers. No. 411, 108 pp.

——, W. S. Benedict, S. A. Clough, D. E. Burch, R. F. Calfee, K. Fox, L. S. Rothman and J. S. Garing, 1973: AFCRL atmospheric absorption line parameters compilation. AFCRL Environ. Res. Papers No. 434, 78 pp.

McDonald, J. E., 1960: Direct absorption of solar radiation by atmospheric water vapor. *J. Meteor.*, **17**, 319–328.

Paltridge, G. W., 1973: Direct measurement of water vapor absorption of solar radiation in the free atmosphere. *J. Atmos. Sci.*, **30**, 156–160.

Sasamori, T., J. London and D. V. Hoyt, 1972: Radiation budget of the Southern Hemisphere. *Meteor. Monogr.*, **13**, No. 35, 9–23.

Tien, C. L., 1968: Thermal radiation properties of gases. *Advances in Heat Transfer*, Vol. 5, Academic Press, 253–324.

Walshaw, C. D., and C. D. Rodgers, 1963: The effect of the Curtis-Godson approximation on the accuracy of radiative heating rate calculations. *Quart. J. Roy. Meteor. Soc.*, **92**, 122–130.

Yamamoto, G., 1962: Direct absorption of solar radiation by atmospheric water vapor, carbon dioxide and molecular oxygen. *J. Atmos. Sci.*, **19**, 182–188.